Monthly Notices of the ROYAL ASTRONOMICAL SOCIETY

MNRAS **482,** 4397–4407 (2019) doi:10.1093/mnras/sty2975
Advance Access publication 2018 November 3

Thermonuclear X-ray bursts in rapid succession in 4U 1636–536 with *AstroSat*-LAXPC

Aru Beri,[1,2,3★] Biswajit Paul,[3] J. S. Yadav,[4] H. M. Antia,[4] P. C. Agrawal,[5] R. K. Manchanda,[6] Dhiraj Dedhia,[5] Jai Verdhan Chauhan,[5] Mayukh Pahari,[2] Ranjeev Misra,[7] Tilak Katoch,[4] P. Madhwani,[4] Parag Shah,[4] Varun[3] and Sujay Mate[3,8]

[1]*DST-INSPIRE Faculty, Indian Institute of Science Education and Research (IISER) Mohali, Punjab 140306, India*
[2]*Physics & Astronomy, University of Southampton, Southampton, Hampshire SO17 1BJ, UK*
[3]*Raman Research Institute, Sadashivnagar, C. V. Raman Avenue, Bangalore-560 080, India*
[4]*Tata Institute of Fundamental Research, Homi Bhabha Road, Mumbai 400005, India*
[5]*UM-DAE Center of Excellence for Basic Sciences, University of Mumbai, Kalina, Mumbai 400098, India*
[6]*University of Mumbai, Kalina, Mumbai 400098, India*
[7]*Inter-University Center for Astronomy and Astrophysics, Ganeshkhind, Pune 411007, India*
[8]*IRAP, Université de Toulouse, CNRS, UPS, CNES, Toulouse, France*

Accepted 2018 October 30. Received 2018 October 29; in original form 2018 April 6

ABSTRACT

We present results from an observation of the low-mass X-ray binary 4U 1636–536 obtained with the *LAXPC* instrument aboard *AstroSat*. The observations of 4U 1636–536 made during the performance verification phase of *AstroSat* showed seven thermonuclear X-ray bursts in a total exposure of ∼65 ks over a period of about two consecutive days. Moreover, the light curve of 4U 1636–536 revealed the presence of a rare triplet of X-ray bursts, having a wait time of about 5.5 min between the second and the third bursts. We also present results from time-resolved spectroscopy performed during these seven X-ray bursts. In addition, we have also detected a transient quasi-periodic oscillation at ∼5 Hz. However, we did not find any evidence of kilo-hertz quasi-periodic oscillations and/or X-ray burst oscillations, perhaps due to the hard spectral state of the source during this observation.

Key words: accretion, accretion discs – stars: neutron – X-rays: binaries – X-rays: bursts – X-rays: individual: 4U 1636–536.

1 INTRODUCTION

Thermonuclear X-ray bursts (also known as Type-I X-ray bursts) are eruptions in X-rays that can be observed from neutron star (NS) low-mass X-ray binaries (LMXBs). These are triggered in the NS envelope due to unstable thermonuclear burning of hydrogen and helium accreted from a low-mass stellar companion (e.g. Woosley & Taam 1976; Schatz et al. 1998). During thermonuclear X-ray bursts, the X-ray luminosity increases many times of the persistent level (for reviews, see Lewin, van Paradijs & Taam 1993; Strohmayer & Bildsten 2006; Galloway et al. 2008). Within a few tens of seconds $10^{38} - 10^{39}$ erg of energy is released. We do not discuss herein long bursts and superbursts that are comparatively more energetic, $10^{40} - 10^{42}$ erg (for details see in 't Zand 2011).

It is believed that most of the accreted fuel is burned during a burst. Therefore, the atmosphere must be completely replaced before a new burst can ignite (see e.g. Woosley et al. 2004; Fisker, Schatz & Thielemann 2008). X-ray bursts with a recurrence time of hours to days have been detected from over 100 sources in our Galaxy [1] (see e.g. Lewin et al. 1993; Strohmayer & Bildsten 2006; Galloway et al. 2008). However, bursts having short recurrence times varying between ∼3 and 45 min have been observed from 15 sources (see Keek et al. 2010 for details).

A large fraction of X-ray burst studies have been done with the PROPORTIONAL COUNTER ARRAY (PCA) aboard *Rossi X-ray Timing Explorer* (*RXTE*) (see e.g. Galloway et al. 2008). The shortest recurrence time reported by Galloway et al. (2008) in *RXTE*-PCA light curves is ∼6.4 min. Linares et al. (2009) later reported a short recurrence time of 5.4 min using *RXTE* observations of 4U 1636–536. Keek et al. (2010) reported the shortest recurrence time between X-ray bursts from 4U 1705–44 to be ∼3.8 min. There also exist an exceptional source, IGR J17480–2446, that showed large number of recurring X-ray bursts during its outburst in 2010. During this outburst, X-ray bursts with recurrence time as short as 3.3 min

★ E-mail: a.beri@soton.ac.uk, aruberi@iisermohali.ac.in

[1] https://www.sron.nl/ jeanz/bursterlist.html

were also observed (Motta et al. 2011; Linares et al. 2012). A study carried out by Boirin et al. (2007) using a long X-ray observation of EXO 0748–676 with the *XMM–Newton* observatory discovered short recurrence time (8–20 min) bursts. The same authors showed that short recurrence time bursts are less energetic compared to the 'normal' recurrence times (few hours). They also found that short recurrence time bursts have peak temperature low in compared to the 'normal' recurrence time bursts and the profiles of such bursts lack 50–100 s long tail. An extensive study carried out by Galloway et al. (2008) using *RXTE* data of 48 accreting NSs revealed that the short recurrence time bursts in many other sources also showed a behaviour that is similar to that observed by Boirin et al. (2007).

Several possibilities have been discussed to explain short recurrence time X-ray bursts. For instance, Fisker, Thielemann & Wiescher (2004) suggested a waiting point in the chain of nuclear reaction network. Very recently, Keek & Heger (2017) proposed an alternative model that shows that there are left overs of the accreted material after the previous X-ray event and these are transported by convection to the ignition depth, producing short recurrence time burst.

The Large Area X-ray Proportional Counter (LAXPC) instrument on-board the Indian multi-wavelength mission *AstroSat* has timing capabilities similar to that of PCA aboard *RXTE* but has a larger effective area at higher energies (see the next section for details). Verdhan Chauhan et al. (2017) and Bhattacharyya et al. (2018) reported detections of thermonuclear X-ray bursts in the LMXB 4U 1728–34. These authors also showed the presence of burst oscillations during the X-ray burst.

4U 1636–536, an extraordinary (most luminous) atoll source (Hasinger & van der Klis 1989), which exhibits a wide variety of X-ray bursts such as double-peaked X-ray bursts (Sztajno et al. 1985; Bhattacharyya & Strohmayer 2006), triple-peaked X-ray bursts (van Paradijs et al. 1986; Zhang et al. 2009), superbursts (Wijnands 2001; Kuulkers et al. 2004), short recurrence time bursts (Keek et al. 2010), was observed with LAXPC as a part of the performance verification. In this work, we report results obtained from the observations of 4U 1636–536 with the LAXPC instrument. We found a total of seven thermonuclear X-ray bursts in these observations of 4U 1636–536 and in particular, we observed the presence of short recurrence time bursts (a rare triplet). We also present the results obtained from the time-resolved spectroscopy performed during X-ray bursts. This is a technique which is often employed for the measurement of NS parameters such as its radius (see e.g. Lewin et al. 1993; Galloway et al. 2008; Bhattacharyya 2010, for details).

2 OBSERVATIONS

2.1 *AstroSat*-LAXPC

AstroSat is the first Indian multi-wavelength astronomical satellite launched on 2015 September 28. It has five instruments on-board (Agrawal 2006; Paul 2013). LAXPC is one of the primary instruments aboard. LAXPC consists of three identical proportional counters with a total effective area of $\sim$6000 cm^2 at 15 keV. The LAXPC detectors have a collimator with a field of view of about $1^\circ \times 1^\circ$. Each LAXPC detector independently records the time of arrival of each photon with a time resolution of 10 μs. The energy resolution at 30 keV is about 15 per cent, 12 per cent, 11 per cent for LAXPC10, LAXPC20 and LAXPC30, respectively (Yadav et al. 2016; Antia et al. 2017).

The three proportional counters of LAXPC are named as LAXPC10, LAXPC20 and LAXPC30. LAXPC detectors work in an energy range of 3–80 keV. Each proportional counter unit has five layers, each with 12 detector cells (for details see Yadav et al. 2016; Antia et al. 2017).

Table 1. LAXPC observation details of 4U 1636–536 starting from MJD 57433.25. In this LAXPC observation, other than the data gaps due to satellite passage through the SAA region and occultation of the source by the Earth, there was some additional data gap in orbit no 02092, around 90 000 s (Fig. 2).

Orbit number	On-source exposure (s)
02078	1925
02079	2769
02080	2764
02081	2776
02082	2771
02083	2764
02084	2392
02085	2815
02086	3239
02087	3662
02088	3851
02089	3741
02090	3303
02091	2779
02092	736
02093	2357
02094	2394
02095	2737
02096	2739
02097	2733
02098	2436
02099	2862

2.2 Data

LAXPC data were collected in two different modes: Broad Band Counting (BBC) and Event Analysis mode (EA). Data collected in the event mode of LAXPC contain information about the time, anodeID and Pulse Height (PHA) of each event. Therefore, we have used EA mode data for the timing and spectral analysis. As a part of the performance verification, *AstroSat* observed thermonuclear X-ray burst source 4U 1636–536 covering 22 orbits during 2016 February 15–16. Observation details are given in Table 1.

3 RESULTS

3.1 Light curves

The *Swift*/Burst Alert Telescope (BAT) is a hard X-ray transient monitor which observes $\sim$88 per cent of the sky each day and provides near real-time coverage of the X-ray sky in the energy range 15–50 keV (Krimm et al. 2013). We have used *Swift*-BAT light curve of 4U 1636–536 to determine the spectral state of this source (see Fig. 1). The BAT light curve of 4U 1636–536 has been binned with a binsize of 1 day. The BAT light curve of 4U 1636–536 shows the long-term variability of about 40 days from 2015 March to 2016 November. Since BAT is a hard X-ray monitor therefore the peak of the light curve (high value of flux in 15–50 keV band) would suggest the hard spectral state of a source.

Fig. 2 shows 3–80 keV light curve of 4U 1636–536 obtained using the data of LAXPC. We plot light curve of each detector

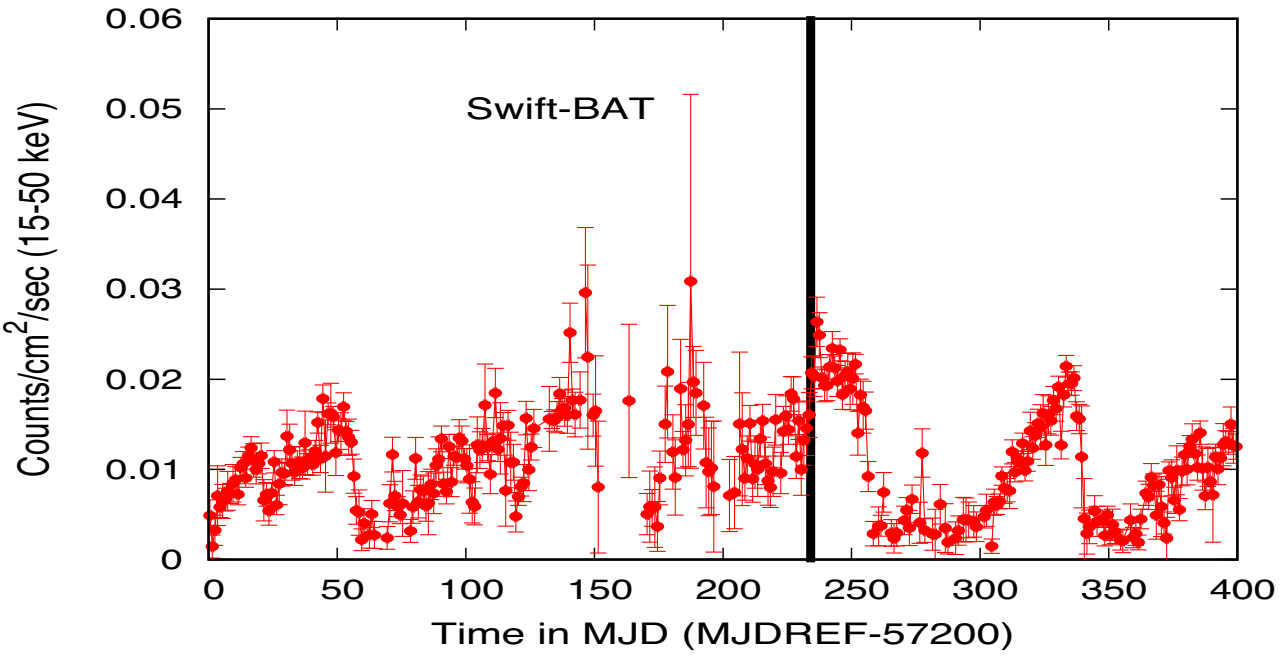

Figure 1. This plot highlights the spectral state of the source during the LAXPC observation using *Swift*-BAT light curve in 15–50 keV band. Thick bold line indicates the time of the LAXPC observation (around 57433 MJD). This figure shows that LAXPC observation was made during the hard state of 4U 1636–536.

separately to demonstrate the identical nature of light curves in the three detectors of LAXPC.

For creating the light curve of 4U 1636–536 with LAXPC, we have used data from all the layers of all the three proportional counter units of LAXPC. Good time intervals (GTI) based on the following filtering criteria, i.e. elevation angle from Earth horizon greater than 2°, Charged Particle Monitor (CPM; Rao et al. 2017) count rate less than 12 counts s^{-1} and angle offset less than 0°.22, were used to create the source light curves. We have used the LAXPC tool task '*lxplc*' for the extraction of light curve. *lxplc* tool allows selection of events based on layers and energy channels. We have used channels ranging from 25 to 611 of each layer for the extraction of light curves of LAXPC10, channels 27–646 for LAXPC30 while we have used channels 20-484 for the extraction of light curve using data from LAXPC20 (which has lower gain compared to LAXPC10, LAXPC30; Antia et al. 2017). The light curves were binned with a binsize of 1 s. Light curve of each proportional counter unit consists of a persistent emission separated by data gaps and seven thermonuclear X-ray bursts. Data gaps in the observation corresponds to times during the Earth occultation and the satellite passing through the South Atlantic Anomaly (SAA) region. The light curves show nearly a constant total count rate of about 414 counts s^{-1}, 320 counts s^{-1}, 327 counts s^{-1} over the entire duration in LAXPC10, LAXPC20, LAXPC30, respectively, except during the seven thermonuclear X-ray bursts observed. The average count rate in LAXPC10, LAXPC20, LAXPC30 measured during the earth occultation is 221 counts s^{-1}, 147 counts s^{-1}, 137 counts s^{-1}, respectively, which accounts for most of the background.

The X-ray bursts observed were found in the data of orbits, viz. 02084, 02087, 02091, 02094 and 02099. The zoomed-in version of these X-ray bursts in each LAXPC unit is shown in the Appendix (Appendix A).

3.2 A triplet of X-ray bursts

We have found a very rare triplet of X-ray bursts in the light curve (see Fig. 3). This triplet was seen in the last orbit of the observation. To estimate the time difference or the wait time between two X-ray events in a triplet, we followed the definition of Boirin et al. (2007). These authors defined wait time of a burst as the separation between its peak time and the peak time of the previous burst. The wait time between two X-ray bursts, namely burst 1 and burst 2 of the triplet, is $\sim$ 7 min while the wait time between the last and the second burst (burst 3 and burst 2 of the triplet) is about 5.5 min.

3.3 Energy-resolved burst profiles

To observe the energy dependence of these X-ray bursts, we created light curves during an X-ray burst in five different narrow energy bands, namely 3–6 keV, 6–12 keV, 12–18 keV, 18–24 keV and 24–30 keV. The light curves were created using data from all layers of three counters of LAXPC and with a binsize of 1 s. Fig. 4 shows an energy-resolved light curve of the burst 1 seen in the observation of 4U 1636–536. For the light curve in the 24–30 keV band, the count rates have been multiplied by a factor of 5 for the visual clarity. This figure indicates that bursts are detected up to 30 keV. We extracted light curves above 30 keV to investigate the effect of bursts on the light curves at higher energies. Light curves created in the 30–80 keV band showed the presence of a dip. The dip observed in the light curves was similar to the some reports of dip observed in hard X-rays during bursts in other sources (Maccarone & Coppi 2003; Chen et al. 2013; Kajava et al. 2017). However, dip observed in the *LAXPC* light curves could also be due to the deadtime effect and to investigate this we corrected hard X-ray light curve for the total count rate in each detector. The count rates were scaled by applying

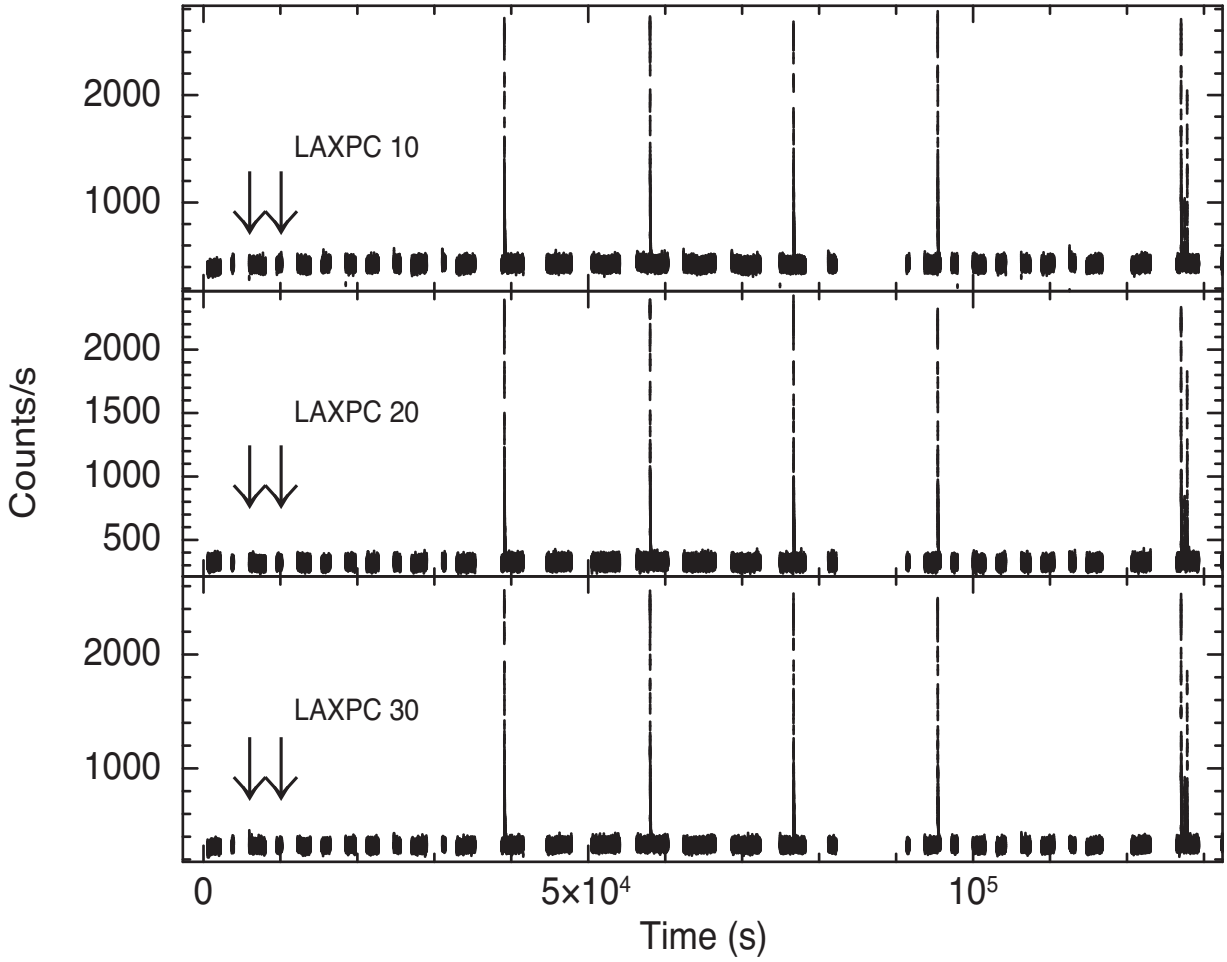

Figure 2. 3–80 keV light curve created using LAXPC data of 4U 1636–536. Light curve is binned with a binsize of 1 s. The arrows indicate the segments of the light curve that show a low-frequency QPO.

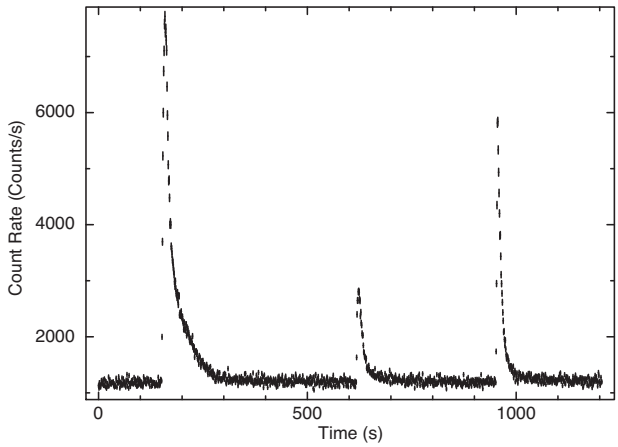

Figure 3. 3–80 keV light curve created using data from the three proportional counters of LAXPC. This plot shows the triplet of X-ray bursts (burst 5, burst 6 and burst 7). Light curve is binned with a binsize of 1 s.

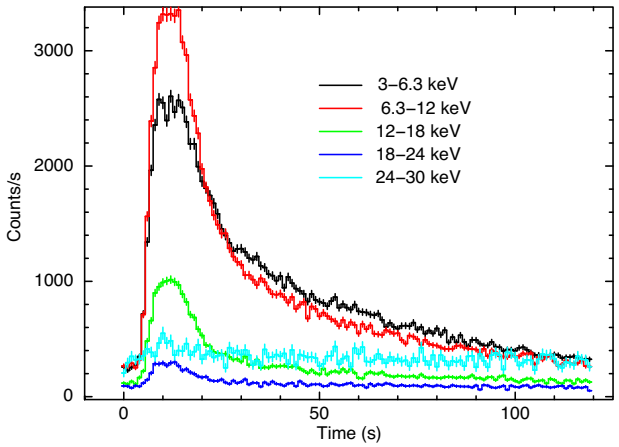

Figure 4. This plot shows a thermonuclear X-ray burst as observed in different energy bands. We have used data during burst 1. This figure shows that the X-ray burst is detected up to 30 keV.

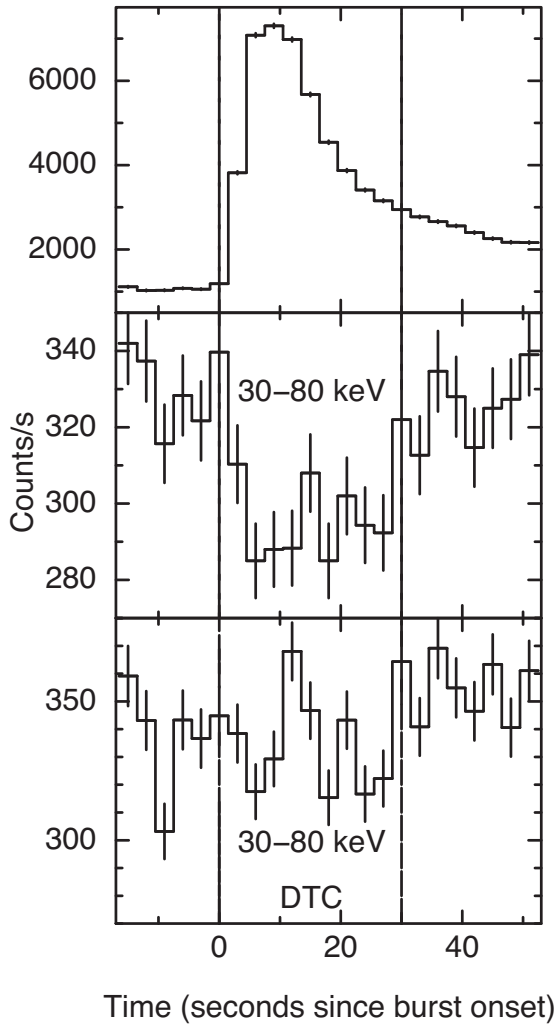

Figure 5. This plot shows that the dip observed in the energy band of 30–80 keV close to the peak of thermonuclear X-ray burst (burst 1) disappears after performing deadtime correction. The light curves are binned with a binsize of 3 s.

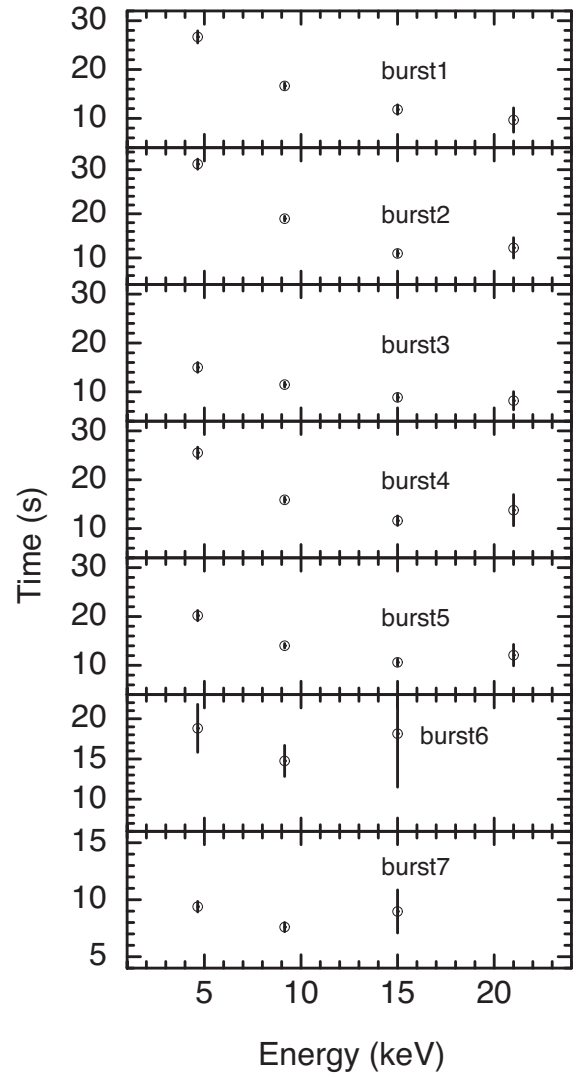

Figure 6. This plot shows an exponential decay time-scales observed in different energy bands during seven bursts observed in the LAXPC data of 4U 1636–536.

appropriate deadtime correction.[2] We observed after applying this correction the dip disappeared (see Fig. 5).

We also noticed the energy dependence of the burst duration in Fig. 4. Therefore, we measured the energy dependence of the burst duration in all the seven X-ray bursts. To measure the exponential decay times during each energy-resolved burst profile we fitted the burst profiles with the QDP model '*burs*'. We found that there is a gradual decrease in the decay time with an increase in energy. Decay time of an X-ray burst varied between ∼28 and 10 s (Fig. 6). A gradual decrease in the temperature due to cooling of burning ashes along the burst decay is the cause of observed energy dependence of burst duration (see e.g. Degenaar et al. 2016).

3.4 Time-resolved spectroscopy

We observed from the energy-resolved light curves that X-ray bursts are detected only up to 30 keV (see Fig. 4). In LAXPC, the soft and medium energy X-rays do not reach the bottom layers of the detectors. Therefore, we have performed time-resolved spectroscopy using single events from the top layer (L1, L2) of each detector of LAXPC. This was done to minimize the background. Each proportional counter has a different energy response file based on various factors gain, quantum efficiency, energy resolution, etc. The gain of the LAXPC detector may vary from observation to observation; therefore we first estimated the gain of each detector of LAXPC using the tool '*k-events-spec*'. We found that during the entire observations the value of gain compared to ground calibration data was ∼1.0, ∼0.99, ∼1.05 for LAXPC10, LAXPC20, LAXPC30, respectively. Based on all these necessary checks we selected an appropriate response file needed while performing spectroscopy. Additional care was taken about the deadtime correction. We modified the value of '*backscal*' keyword of each time-resolved spectra. The value was calculated using $1.0/(1.0 - N \times t)$, where N is the count rate and t is measured deadtime (∼42.3 μs).

In order to investigate spectral evolution during X-ray bursts, the spectra during X-ray bursts were extracted using a time interval of 1 s. For each burst, we extracted the spectrum using 16 s of data preceding the burst. This was subtracted for all burst intervals as the underlying accretion emission and background.

[2] http://www.rri.res.in/ rripoc/

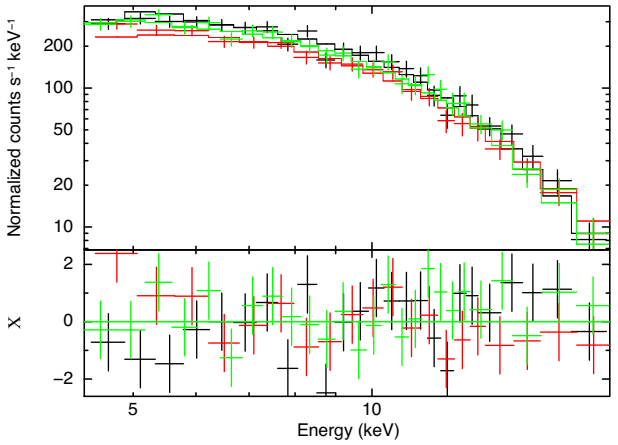

Figure 7. An example best-fitting count rate spectrum of 4U 1636–536 obtained using the simultaneous spectral fitting of the data of three detectors of LAXPC. The lower panel shows the residuals of the fit, where χ is defined as $(x_i\text{-}x_m)/\sigma_i$. x_i and σ_i correspond to the observed counts and associated uncertainty while x_m is the model prediction.

The net burst spectra in 4–20 keV band were fitted in XSPEC (Arnaud 1996), using a blackbody model 'BBODYRAD' consisting of two parameters, a temperature (T_{BB}) and a normalization ($K = (R_{BB}/d_{10})^2$), where R_{BB} is the blackbody radius and d_{10} is the source distance in units of 10 kpc. To account for interstellar extinction, we used the 'TBABS' model component (Wilms, Allen & McCray 2000). Since hydrogen column density is not well constrained in the LAXPC energy band, therefore we fixed $N_{\rm H} = 0.25 \times 10^{22}$ cm^{-2} (Galloway et al. 2008). Fig. 7 shows an example count rate spectrum fitted with a blackbody model attenuated with an interstellar absorption component. While performing the spectral fitting we have also added a systematic error of 1 per cent to the time-resolved spectra.

In Fig. 8, we show the best-fitting parameters obtained after performing time-resolved spectroscopy of the seven bursts. The top panel of each plot shows count rate during an X-ray burst, the second panel shows the temperature evolution and the third panel shows the blackbody normalization during each short segment of an X-ray burst. Flux estimated in 4–20 keV band is shown in the fourth panel of each plot while the fifth and the sixth panels show the reduced chi-squared obtained from each spectral fitting and the radius measured from the values of blackbody normalization, respectively. We have not applied the correction factors such as colour correction factor for the measurement of a real value of NS radius. The maximum temperature observed in an X-ray burst 1 is 2.47 ± 0.05 keV. The emission radii inferred from the blackbody normalization spectral fit suggest that it is a Photospheric radius Expansion X-ray burst. Nearly same value of maximum temperature was also seen in bursts 2, 3, 4 and 5. However, we notice a lower value of maximum temperature (∼1.7 keV) in last two bursts of the triplet.

3.5 Power density spectrum

We have added light curves from all the three detectors of LAXPC to generate the power density spectra of 4U 1636–536. To have a high ratio of the source to the background count rate, we have used data from the top two layers and restricted the light curves to 3–25 keV band.[3] We searched for both low- and high-frequency QPOs in the light curves excluding X-ray bursts. For the case of low-frequency QPOs we used the light curves binned with a binsize of 1 ms while for the high-frequency QPO search we used light curves having binsize of 0.1 ms. The light curves were divided into segments each with 8192 bins. PDS from all the segments were averaged to produce the final PDS. Fig. 9 shows the presence of a weak low-frequency QPO-like feature around 5 Hz observed in the light curve of one of the orbits (02079). However, the Q-factor of this QPO-like feature is low, ∼1.2. We also searched for the presence of milli-hertz QPOs in the light curves of each orbit separately; however, we did not find the presence of any such feature in the PDS. On the right hand side of Fig. 9, we show the PDS obtained after using light curves from all the orbits. This covers wide range of frequency 1–5000 Hz. We also attempted to search for burst oscillations using light curves during the X-ray bursts; however, we did not find any burst oscillations around the previously observed burst oscillation feature at 580 Hz (Strohmayer & Markwardt 2002).

4 DISCUSSIONS

In this work, we have used a long LAXPC observation of 4U 1636–536. The light curve of 4U 1636–536 revealed the presence of seven X-ray bursts. Last orbit of the observation showed a triplet of X-ray bursts. Triplets of X-ray bursts are rare events. Therefore, we searched the literature and found that a total of 19 triplets of X-ray bursts have been observed so far from sources other than 4U 1636–536. The wait time between the three bursts of these X-ray triplets is less than 30 min (Table 2). In particular, EXO 0748–676 showed X-ray bursts having wait times of ∼12 min between the three bursts of triplets (Boirin et al. 2007).

4.1 Burst catalogue

Multi-INstrument Burst ARchive (MINBAR) is a collection of Type I bursts that are observed with different X-ray observatories (*RXTE*; *BeppoSAX*, *INTEGRAL*), and that are all analysed in a uniform way. Currently, it contains information on 6987 Type I X-ray bursts from 84 burst sources (MINBAR version 0.9).[4] MINBAR was used to locate *RXTE*-PCA observations of 4U 1636–536 that shows bursts with recurrence times of less than 30 min. Table 3 shows the X-ray burst triplets observed in the *RXTE*-PCA light curves that were not included in Keek et al. (2010). We found two additional triplets of X-ray bursts in 4U 1636–536 which were not reported by Keek et al. (2010). The shortest wait time observed between second and the third bursts of a triplet of X-ray bursts in the *RXTE*-PCA light curves is 7.4 min. However, the shortest wait time observed between first and the second bursts of a triplet in the PCA light curves is ≈8 min. We thus notice that the LAXPC observation of 4U 1636–536 revealed one of the shortest triplets among all the known triplets of X-ray bursts (Table 2) and also the shortest time difference (∼5.5 min) among the triplet of bursts observed in this source (Table 3). Similar wait time was also reported by Linares et al. (2009) during the doublet of X-ray bursts of 4U 1636–536. Several models have been proposed to explain the occurrence of short recurrence bursts. Very recently, Keek & Heger (2017) proposed one-dimensional multi-zone model that reproduces short recurrence bursts on the observed time-scale of minutes. Their

[3] http://www.rri.res.in/∼ rripoc/
[4] http://burst.sci.monash.edu/minbar

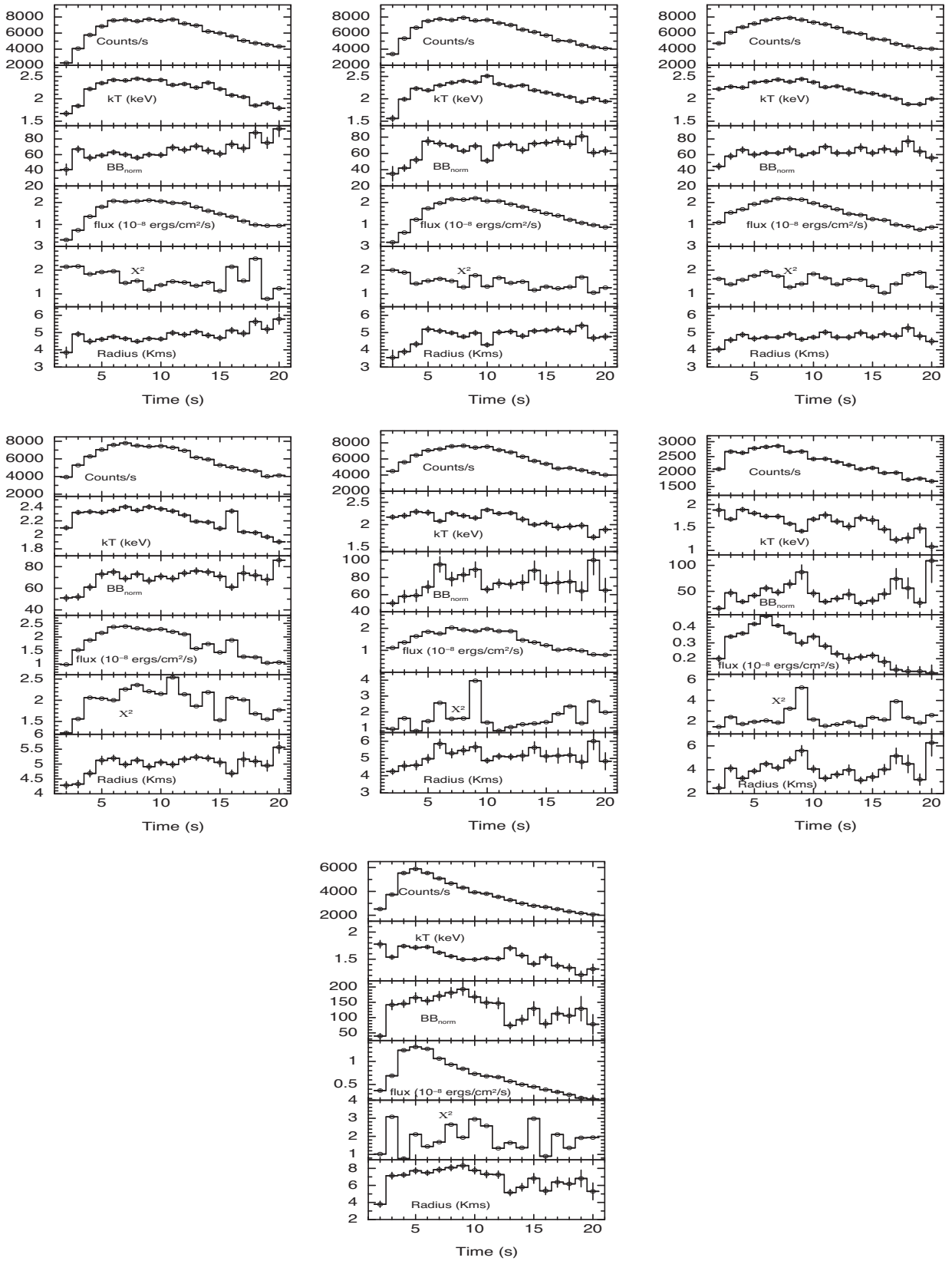

Figure 8. First panel: in the left we show the best-fitting parameters obtained after performing time-resolved spectroscopy of burst 1 .We have not applied correction factors to obtain a real value of the NS radius. Middle: best-fitting parameters obtained after performing time-resolved spectroscopy of burst 2 and the right plot shows the best-fitting parameters obtained from the time-resolved spectroscopy of burst 3. Second panel: In the left we show the best-fitting parameters obtained after performing time-resolved spectroscopy of burst 4, the plot in the middle is for burst 5 while the right plot is for burst 6. Third panel: best-fitting parameters obtained after performing time-resolved spectroscopy of burst 7.

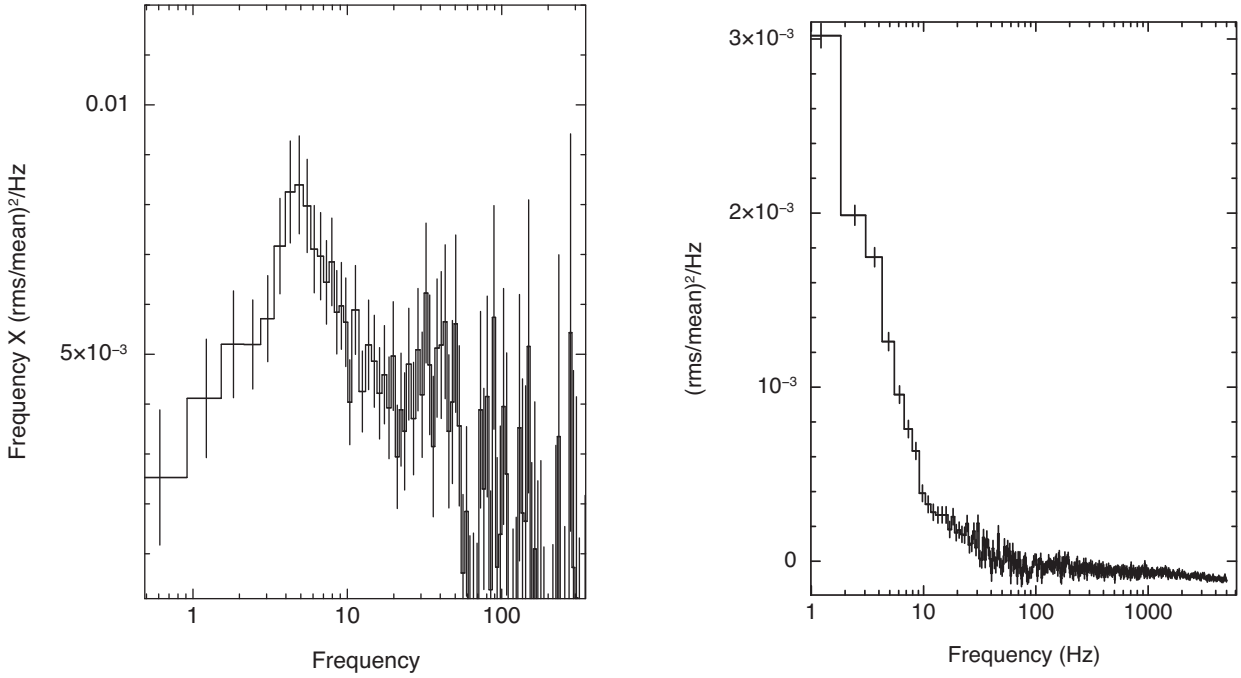

Figure 9. Left: power density spectrum created using combined light curve from LXP1, LXP2 and LXP3 of orbit –02079. Light curves were created using data from the top layers (L1, L2, L3 and L4) and in energy 2.5–25 keV. There exists a weak QPO-like feature around ∼5 Hz (Q-value ∼1.2). Right: we show the PDS covering wide frequency range 1–5000 Hz created using the light curves of binsize 0.1 ms. We have used data of all the detectors of LAXPC and from all the orbits to obtain this PDS.

Table 2. Sources that exhibited a series of three X-ray bursts having recurrence time less than 30 min. We also note that Boirin et al. (2007) reported five X-ray triplets in EXO 0748–676 having wait times of ∼12 min between the three bursts of X-ray triplets.

Source name	Number of triplets
4U 1608–522[a]	1
EXO 1745–248[a]	1
2E 1742.9–2929[a]	3
Rapid burster[a]	4
4U 1705–44[a]	1
2S 1742–294[b]	3
Aql X–1[b]	1
EXO 0748–676[c]	5

Notes.
[a]Galloway et al. (2008).
[b]Keek et al. (2010).
[c]Boirin et al. (2007).

Table 3. Triplet of thermonuclear X-ray bursts observed in 4U 1636–536 with *RXTE* (MINBAR bursts).

Observation ID	Wait times (min) First and second bursts	Wait times (min) Second and third bursts
60032-05-07-01	∼8.4	∼11.6
93087-01-42-10	∼13.8	∼7.4

simulations are based on the convective mixing driven by opacity. The authors proposed that bursts that ignite in a relatively hot NS envelope leave a substantial fraction of unburnt fuel and convective mixing brings this fuel down to the ignition depth on the observed time-scale of minutes. We compared our observational results with that predicted by Keek & Heger (2017). We observe that although the recurrence time-scales match with that obtained by Keek & Heger (2017) but the profile of triple X-ray bursts obtained by these authors does not match the one observed with LAXPC. The authors predicted intermediate bumps between the X-ray bursts which are caused by convection; however, we do not see such bumps in the light curves. Moreover, the X-ray burst in the middle of the triplet is much fainter compared to the other two X-ray bursts in the triplet. This is again not consistent with that predicted by Keek & Heger (2017). Grebenev & Chelovekov (2017) recently studied short recurrence X-ray bursts using the data of *INTEGRAL*. The authors found the profile of triple X-ray bursts similar to that has been observed in 4U 1636–536 using the data of LAXPC. The authors explained these short recurrence bursts based on the model of a spreading layer of accreting matter over the NS surface. However, these authors believe that further refinement in the model is required for the complete understanding of the existence of triple X-ray bursts.

The large effective area of the LAXPC instrument at higher energies allowed us to create the energy-resolved burst profiles. We found that bursts were detected up to 30 keV. Above 30 keV, the raw light curves of LAXPC detectors showed a dip similar to those reported in some other sources (Maccarone & Coppi 2003; Kajava et al. 2017). However, after a deadtime correction, the hard X-ray light curve during the burst was found to be consistent with the pre-burst emission. We observe a strong energy dependence of burst decay times. Decrease in the burst decay times with the increase in energy suggests the cooling of burning ashes.

Time-resolved spectroscopy during X-ray bursts was performed using spectra with 1 s time interval. From the time-resolved spectroscopy we found that the maximum temperature measured is ∼2.5 ± 0.05 keV.

The power density spectral analysis showed the presence of a QPO around 5 Hz. The low-frequency QPO is observed in black holes and in accreting NSs as well as in non-pulsating NSs. The low-frequency QPO covers a wide range between 0.1 and 50 Hz (see Altamirano et al. 2008b, and references therein). Moreover, these authors suggest that the range of low frequency covered in a source is not related to spin frequency, angular momentum or luminosity of the object. We did not detect any kilo-hertz QPOs in this observation of 4U 1636–536. This again suggests hard spectral state of the source as high-frequency QPOs are often observed during the soft spectral state of this source (Belloni et al. 2007). This is well supported by the fact that the *Swift*-BAT light curve suggested that this observation of 4U 1636–536 was made near the peak of its light curve in 15–50 keV band.

The atoll sources are known to display three main tracks in the colour–colour diagram. These three spectral states are: the extreme island state (EIS), the island state (IS) and the banana branch (BB) (Hasinger & van der Klis 1989). Altamirano (2008) has described in detail the characteristics of each of these states. To confirm the hard (island) spectral state of the present LAXPC observation, we have used the colour–colour diagram of 4U 1636–536 (fig. 1 of Altamirano et al. 2008a). The authors defined soft and hard colours as the ratio of count rates in 3.5–6.0 keV/2.0–3.5 keV and 9.7–16.0 keV/6.0–9.7 keV, respectively. They also normalized the colours by the corresponding Crab Nebula colour values that are closest in time to correct for the gain changes as well as for the differences in the effective area between different proportional counters of *RXTE*. We have adapted the same technique to estimate the colours of the LAXPC observation; however, we have used slightly different energy bands for the estimation of colours. For the soft and the hard colours, we used the ratios of count rates in 6.0–9.7 keV/3.0-6.0 keV and 16.0–25.0 keV/9.7–16.0 keV, respectively. It is quite interesting to notice that the LAXPC observation falls on the island branch which corresponds to the hard spectral state (see Fig. 10). We also noticed that all the previous known short recurrence bursts from this source (see e.g. Keek et al. 2010) lie on the island branch of the colour–colour diagram. The observations performed with *RXTE* that exhibit triplets of X-ray bursts (shown in cyan colour in Fig. 10) also lie close to this observation performed with LAXPC.

Altamirano et al. (2008a) showed that close to the transition between the island and the banana state, 4U 1636–536 exhibits milli-hertz quasi-periodic oscillations (mHz QPOs) (see figs 1 and 2 of their paper). We did not detect any milli-hertz oscillations in the power density spectrum created using the LAXPC observation. The non-detection of mHz QPOs further supports the fact that the current observation does not lie close to the transition region between the island and the banana state. It is proposed that mHz QPOs are the consequence of marginally stable burning on the NS surface (Heger et al. 2007). The non-detection of mHz QPOs in the LAXPC observation suggests that the accreted fuel is not available for the stable burning (Altamirano et al. 2008a). This is well supported by the fact that we observe seven consecutive bursts in almost a day-long observation.

To summarize, we present the results obtained with the study of seven thermonuclear X-ray bursts observed with *AsroSat*-LAXPC. The short recurrence time bursts (a rare triplet) in the LMXB 4U 1636–536 have been detected for the first time with *AsroSat*-LAXPC. We have shown the energy dependence of burst profiles and have also discussed the caveats due to the background at higher energies. This paper along with two other papers on thermonuclear X-ray bursts observed with LAXPC (Verdhan Chauhan et al. 2017; Bhattacharyya et al. 2018) demonstrates the sensitivity of the LAXPC instrument to detect and study thermonuclear X-ray bursts.

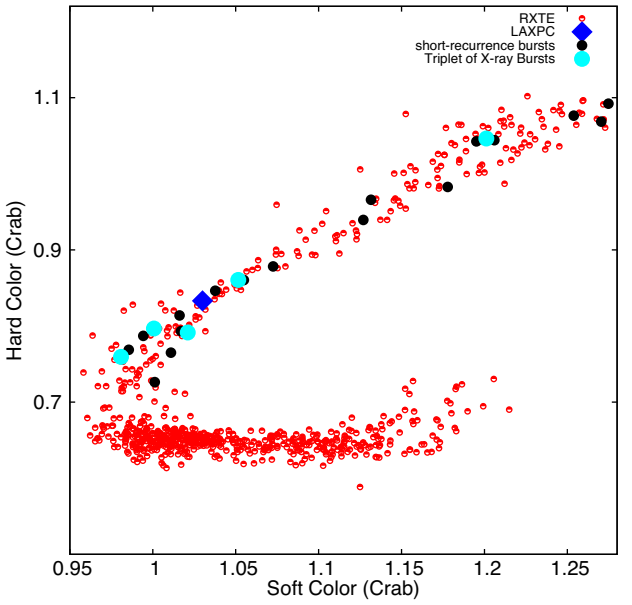

Figure 10. Colour–colour diagram of 4U 1636–536 adapted from Altamirano et al. (2008a). (See text for the details about the energy bands used for the estimation of soft and hard colours.). This figure highlights the position of LAXPC observation of 4U 1636–536 in the colour–colour diagram. The observations performed with the RXTE observatory that showed short recurrence X-ray bursts in this source are also shown.

ACKNOWLEDGEMENTS

AB and MP gratefully acknowledge the Royal Society and SERB (Science & Engineering Research Board, India) for financial support through Newton-Bhabha Fund. AB is supported by an INSPIRE Faculty Grant (DST/INSPIRE/04/2018/001265) by the Department of Science and Technology, Government of India. AB thanks Dr Diego Altamirano for providing the RXTE data for Fig. 10, and for useful discussions. We acknowledge strong support from Indian Space Research Organization (ISRO) in various aspect of *LAXPC* instrument building, testing, software development and mission operation during payload verification phase. This paper uses preliminary analysis results from the MINBAR, which is supported under the Australian Academy of Science's Scientific Visits to Europe program, and the Australian Research Council's Discovery Projects and Future Fellowship funding schemes. We also thank Dr Laurens Keek for providing information on bursts that were not included in their paper (Keek et al. 2010).

REFERENCES

Agrawal P. C., 2006, Adv. Space Res., 38, 2989
Altamirano D., 2008, PhD thesis, Sterrenkundig Instituut 'Anton Pannekoek' University of Amsterdam
Altamirano D., van der Klis M., Wijnands R., Cumming A., 2008a, ApJ, 673, L35
Altamirano D., van der Klis M., Méndez M., Jonker P. G., Klein-Wolt M., Lewin W. H. G., 2008b, ApJ, 685, 436
Antia H. M. et al., 2017, ApJS, 231, 10

Arnaud K. A., 1996, in Jacoby G. H., Barnes J., eds, ASP Conf. Ser. Vol. 101, Astronomical Data Analysis Software and Systems V. Astron. Soc. Pac., San Francisco, p. 17
Belloni T., Homan J., Motta S., Ratti E., Méndez M., 2007, MNRAS, 379, 247
Bhattacharyya S., 2010, Adv. Space Res., 45, 949
Bhattacharyya S., Strohmayer T. E., 2006, ApJ, 636, L121
Bhattacharyya S. et al., 2018, ApJ, 860, 88
Boirin L., Keek L., Méndez M., Cumming A., in't Zand J. J. M., Cottam J., Paerels F., Lewin W. H. G., 2007, A&A, 465, 559
Chen Y.-P., Zhang S., Zhang S.-N., Ji L., Torres D. F., Kretschmar P., Li J., Wang J.-M., 2013, ApJ, 777, L9
Degenaar N., Koljonen K. I. I., Chakrabarty D., Kara E., Altamirano D., Miller J. M., Fabian A. C., 2016, MNRAS, 456, 4256
Fisker J. L., Thielemann F.-K., Wiescher M., 2004, ApJ, 608, L61
Fisker J. L., Schatz H., Thielemann F.-K., 2008, ApJS, 174, 261
Galloway D. K., Muno M. P., Hartman J. M., Psaltis D., Chakrabarty D., 2008, ApJS, 179, 360
Grebenev S. A., Chelovekov I. V., 2017, Astron. Lett., 43, 583
Hasinger G., van der Klis M., 1989, A&A, 225, 79
Heger A., Cumming A., Galloway D. K., Woosley S. E., 2007, ApJ, 671, L141
in 't Zand J., 2011, preprint (arXiv:1102.3345)
Kajava J. J. E., Sánchez-Fernández C., Kuulkers E., Poutanen J., 2017, A&A, 599, A89
Keek L., Heger A., 2017, ApJ, 842, 113
Keek L., Galloway D. K., in't Zand J. J. M., Heger A., 2010, ApJ, 718, 292
Krimm H. A. et al., 2013, ApJS, 209, 14
Kuulkers E., in't Zand J., Homan J., van Straaten S., Altamirano D., van der Klis M., 2004, in Kaaret P., Lamb F. K., Swank J. H., eds, AIP Conf. Ser. Vol. 714, X-ray Timing 2003: Rossi and Beyond. Astron. Soc. Pac., San Francisco,p. 257
Lewin W. H. G., van Paradijs J., Taam R. E., 1993, Space Sci. Rev., 62, 223
Linares M. et al., 2009, Astron. Telegram, 1979
Linares M., Altamirano D., Chakrabarty D., Cumming A., Keek L., 2012, ApJ, 748, 82
Maccarone T. J., Coppi P. S., 2003, A&A, 399, 1151
Motta S. et al., 2011, MNRAS, 414, 1508
Paul B., 2013, Int. J. Modern Phys. D, 22, 1341009
Rao A. R. et al., 2017, J. Astrophys. Astron., 38, 33
Schatz H. et al., 1998, Phys. Rep., 294, 167
Strohmayer T., Bildsten L., 2006, New Views of Thermonuclear Bursts. Cambridge Univ. Press, Cambridge, UK, p. 113
Strohmayer T. E., Markwardt C. B., 2002, ApJ, 577, 337
Sztajno M., van Paradijs J., Lewin W. H. G., Trumper J., Stollman G., Pietsch W., van der Klis M., 1985, ApJ, 299, 487
van Paradijs J., Sztajno M., Lewin W. H. G., Trumper J., Vacca W. D., van der Klis M., 1986, MNRAS, 221, 617
Verdhan Chauhan J. et al., 2017, ApJ, 841, 41
Wijnands R., 2001, ApJ, 554, L59
Wilms J., Allen A., McCray R., 2000, ApJ, 542, 914
Woosley S. E., Taam R. E., 1976, Nature, 263, 101
Woosley S. E. et al., 2004, ApJS, 151, 75
Yadav J. S. et al., 2016, Proc. SPIE, 9905, 99051D
Zhang G., Méndez M., Altamirano D., Belloni T. M., Homan J., 2009, MNRAS, 398, 368

APPENDIX A: THERMONUCLEAR X-RAY BURSTS AS SEEN IN THREE PROPORTIONAL COUNTER UNITS OF LAXPC

Here, we show burst profiles as seen in different proportional counters of LAXPC. The light curves were binned with a binsize of 1 s. The count rates and profile shapes are consistent in all the detectors.

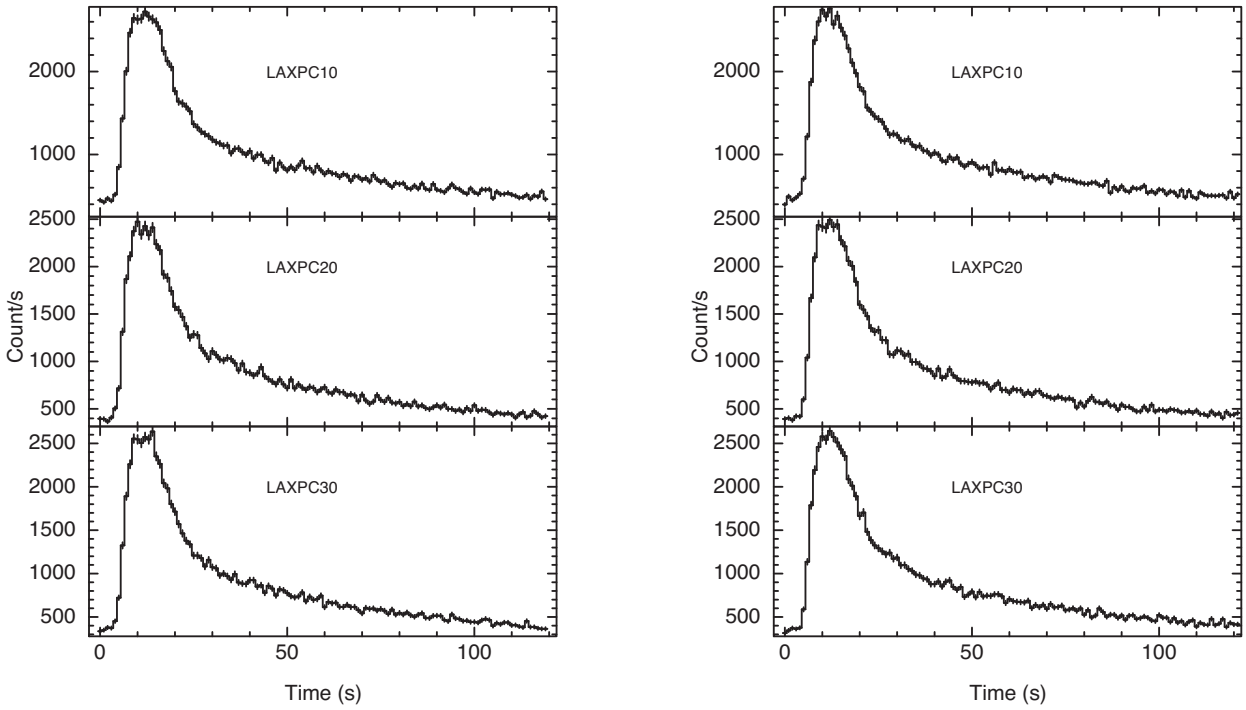

Figure A1. Left: the first thermonuclear X-ray burst (burst 1) as seen in the three detectors of LAXPC. Right: the second X-ray burst (burst 2) observed in this observation of 4U 1636–536.

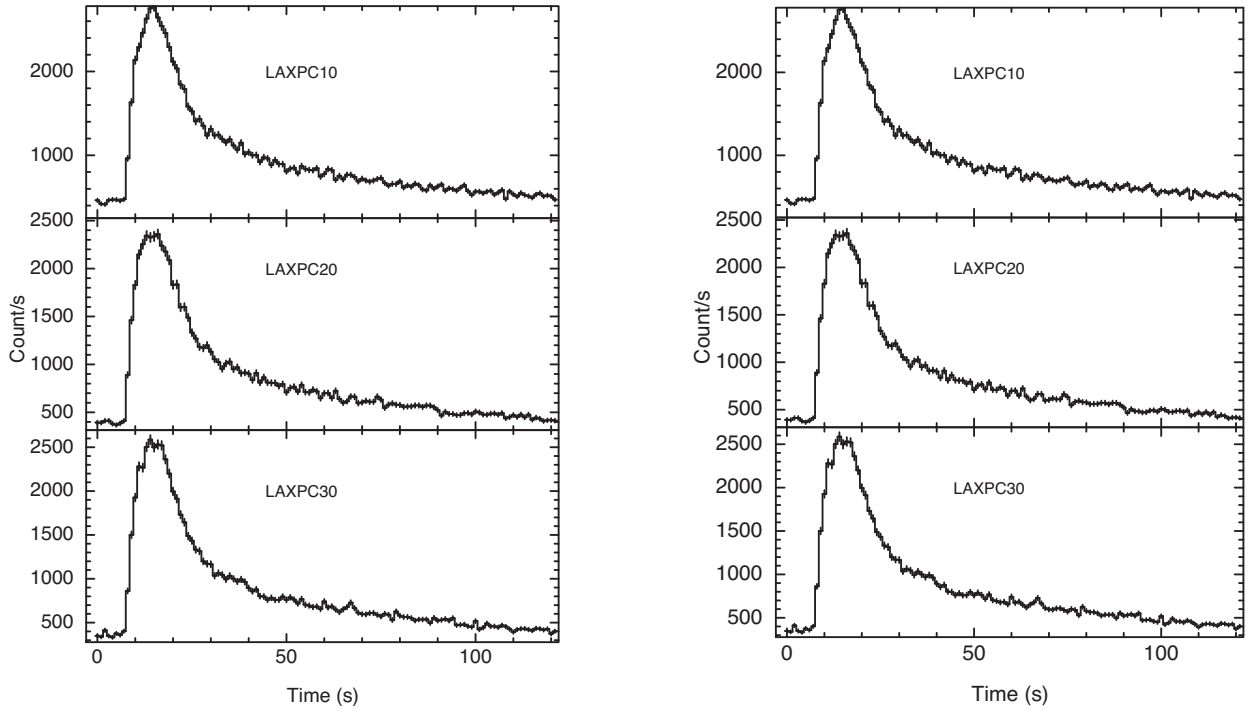

Figure A2. Left: thermonuclear X-ray burst (burst 3) as observed with the three detectors of LAXPC. Right: the fourth X-ray burst (burst 4) as observed with the three detectors of LAXPC.

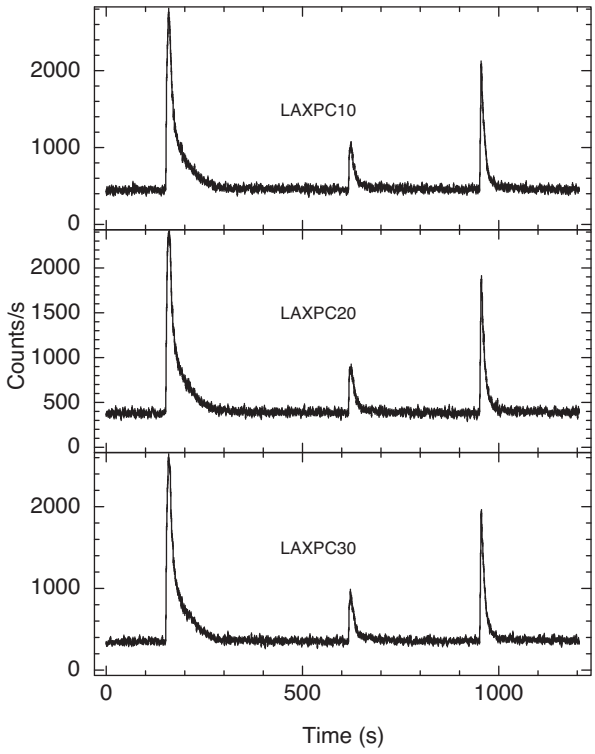

Figure A3. The triplet of X-ray bursts seen in the observation of 4U 1636–536.

This paper has been typeset from a TEX/LATEX file prepared by the author.